A Directed Evolution-Derived Chimeric Receptor Displaying a Natural Killer Receptor Repertoire Exhibits Pan-cancer Cytotoxicity

Yaqi Gao, Xudong Tang, Xinyu Zhu, Song Zhang, Yinran Luo, Xiaoyuan Chen, Hanyue Liu, Jianhua Luo*, Meng Guo*

*Correspondence to: Jianhua Luo (luojh@immunol.org), Meng Guo (guom@immunol.org)

Abstract

CAR-NK cells embody a cutting-edge approach for cancer immunotherapy. Despite their potential, solid tumors frequently present clonal heterogeneity and a deficiency in lymphocyte activation signals, impeding NK cell proliferation and cytotoxic effectiveness. To address this, we developed a novel class of chimeric receptors through charge-induced oligomerization (eCAR). This system incorporates a second-generation CAR design featuring positively charged transmembrane regions paired with negatively charged transmembrane domains equipped with IL2Rβ and/or IL2Rγ intracellular domains. eCAR is proved to enhance tumor antigen-dependent lymphocyte proliferation and activation. Further, we integrated NKR library as a sensor within eCAR structure, which was expressed in NK-92 cells. This engineered cell library demonstrated ligand-dependent cytotoxicity against a broad spectrum of tumor cells and tumor-derived organoids. The study underscores a novel strategy for NK cell-based cancer immunotherapy that exploits an NKR library as a sensor, enabling targeted and efficient destruction of tumor cells across a diverse set of malignancies.

Keywords: Natural killer; NKR repertoire; chimeric receptor; IL-2 signaling; auto-expansion.

Introduction

Immunotherapy has revolutionized clinical treatment strategy, with chimeric antigen receptor natural killer (CAR-NK) cell therapy emerging as a particularly promising approach (*1*). CARs are engineered fusion proteins that integrate an extracellular ligand-binding domain with intracellular signaling domains through a spacer and transmembrane segment, including the CD3ζ immunoreceptor tyrosine-based activation motifs (ITAMs) along with co-stimulatory domains such as 4-1BB, allowing CARs to tap into native signaling pathways that drive NK cell functions like cytokine release and cytotoxicity (*2*).

Despite these advances, the effectiveness of CAR-NK therapies in treating solid tumors is hindered by heterogeneity, complicating the consistent identification and targeting of tumor antigens. Additionally, tumors often foster an immunosuppressive tumor microenvironment (TME), impeding the activation and proliferation of lymphocytes (*3, 4*). This environment, marked by a deficiency in essential cytokines such as IL-2 and IL-15, critically undermines the activation and sustained cytotoxic activity of NK cells (*5, 6*).

One strategy to counteract the tumor's TME involves switching inhibitory signals into activation signals for adoptive cells. For instance, arming adoptive cells with scFv that recognizes PD-L1, linked to co-stimulatory domains, enhances cytotoxic activity targeting PD-L1 expressed tumors (*7*). Nonetheless, NK cells still lack proliferative and cytotoxicity in the TME characterized by an IL-2 deficit. A promising approach is the incorporation of the intracellular portion of IL-2R into the CAR intracellular domain, transforming tumor antigen signals into IL-2R cascade (*7*). Notably, the activation of JAKs/STATs downstream of IL-2R depends on the oligomerization of the β and γ chains (*8*), directly linking the IL-2R intracellular domains into CAR has not been widely demonstrated. Inspiringly, membrane proteins can oligomerize through electrostatic interactions, such as the positive amino acids in the transmembrane regions of natural killer receptor (NKR), which facilitate activating signals by associating with negatively charged residues in transmembrane adaptor proteins containing immunoreceptor tyrosine-based activation motifs (*9*). This feature provides a viable strategy for designing chimeric receptor oligomerization to transduce IL-2 signals.

NK cells exert T-cell receptor (TCR)-independent cytotoxicity primarily through the expression of activating receptors known as killer activation receptors (KARs) (*10*). Ligands of receptors such as NKG2D, NKp30, and DNAX accessory molecule-1 (DNAM-1) are ubiquitously expressed in most solid tumors but are absent in normal cells (*10*), making the extracellular domains of KARs suitable sensors for chimeric receptors. Additionally, tumors often suppress NK cell activity by expressing ligands for killer inhibitory receptors (KIRs) (*11*). Incorporating the extracellular domains of

KIRs as sensors also allows for the conversion of inhibitory signals into activation signals upon tumor antigen stimulation. Utilizing these NKRs to recognize multiple tumor antigens expands the range of inhibition of malignancies.

In this study, we constructed a cellular therapeutic displaying an NKR repertoire through two rounds of directed evolution. In the first evolutionary cycle, using a tumor antigen stimulus in an IL-2-free culture system, we developed an evolutionary CAR (eCAR) structure that enables tumor antigen-dependent NK cell expansion. In the second evolutionary cycle, by presenting an NKR repertoire on the extracellular segment of the eCAR structure, the cells achieved broad-spectrum tumoricidal activity.

Results

Developing CAR Constructs for Tumor Antigen-Dependent Proliferation via Directed Evolution

We engineered two classes of CARs configurations targeting CD19, totaling 23 distinct constructs: the Tandem IL2R-ICD CARs incorporate the intracellular domains (ICDs) of the β and/or γ chains serially linked to CD3ζ; the Charge-attracting IL2R-ICD CARs feature a positively charged transmembrane region connecting 4-1BB and CD3ζ, and a negatively charged transmembrane region linked to the IL2R ICD (Fig. 1a). All CARs are coupled with enhanced green fluorescent protein (EGFP) via an internal ribosome entry site (IRES) to identification (Extended Data Fig. 1). These CAR gene fragments were transduced into NK-92 cells using lentivirus, with a second-generation CD19-targeting CAR-NK (BBζ) serving as a positive control (Fig. 1b). Under IL-2 supplemented culturing conditions, NK92, αCD19 NK cells (termed αCD19), and the αCD19 CAR library exhibited comparable proliferation rates. However, in the absence of IL-2 and upon stimulation by Raji cells (CD19 positive), only the αCD19 CAR library demonstrated significant expansion (Fig. 1c-d). The results indicates that the αCD19 CAR library can robustly proliferate in an IL-2 independent manner, responding exclusively to tumor antigen signals.

To pinpoint the specific sequences within the library that facilitate enhanced NK cell proliferation solely in response to tumor antigens, we repeated stimulate NK cells with Raji cells in an IL-2-deprived environment (Extended Data Fig. 2a-c). Post-stimulation, EGFP-positive NK cells were sorted and subjected to single-cell cloning. Subsequent stimulations with Raji cells led to significant enrichment of the constructs 46-BBζ/Fcγ/3β, 46-BBζ/Fcβ/3γ, and 44-BBζ/12β/12γ in comparison to others (Fig. 1e). These results demonstrate that these specific constructs are exceptionally effective in driving robust NK cell proliferation in response to tumor antigen stimulation, independent of exogenous IL-2. These constructs have been designated as eCAR1, eCAR2, and eCAR3, respectively.

Antigen-Specific Proliferation of eCAR-NK in an IL-2- deprived Environment

We further explored the capacity of eCARs to sustain extensive proliferation in an IL-2 independent environment, relying exclusively on tumor antigen signals. To this end, we engineered CAR-NK cells to target specific antigens associated with different malignancies-CD19 and CD20 for hematological cancers, GPC3 for hepatocellular carcinoma, and MSLN for pancreatic cancer, each can be sensed by corresponding eCAR (Fig. 2a). Experimental results revealed that both αCD19 eCAR1 and αCD19 eCAR2 exhibited robust proliferation in response to stimulation by Raji cells, even in the absence of IL-2 (Fig. 2b). In contrast, coculture with CD19-negative tumor cells (K562) without IL-2 supplementation resulted in no proliferation of both αCD19 eCAR1 and αCD19 eCAR2 (Fig. 2c). These observations affirm that eCAR1 and eCAR2 are capable of extensive proliferation driven solely by tumor antigen signals, independent of IL-2.

Given that the proliferative capabilities of αCD19 eCAR1 and αCD19 eCAR2 were indistinguishable, we chose to further validate eCAR1 and henceforth refer to it as eCAR. Similarly, significant proliferation was observed when αCD20 eCAR and αGPC3 eCAR were exposed to their corresponding target cells-Raji (CD20 positive) for αCD20 eCAR and HepG2 (GPC3 positive) for αGPC3 eCAR (Fig. 2d-e). Additionally, under stimulation by the pancreatic cancer cell line AsPC-1 (MSLN-positive), αMSLN eCAR was able to proliferate, whereas stimulation with MSLN-knockout AsPC-1 cells failed to proliferate (Fig. 2f). We next assessed the IL-2R downstream signaling in eCAR-NK cells upon tumor antigen stimulation. Phosphorylation of JAK1/3-STAT1/3/5 and AKT was effectively induced in eCAR-NK by MSLN-positive AsPC-1 cells, a response that was not replicated in either NK-92 or CAR-NK. This activation of signaling pathways was contingent upon the interaction between the tumor antigen and eCAR; stimulation with MSLN-knockout AsPC-1 did not activate these pathways in eCAR-NK cells (Fig. 2g). These findings highlight the specificity of eCAR in driving targeted signaling responses, crucially dependent on antigen recognition in an IL-2-deprived environment.

Enhanced Cytotoxicity of eCAR-NK in an IL-2-deprived Environments

To deepen our understanding, we proceeded to evaluate the cytotoxic capabilities of eCAR-NK in an IL-2-deprived environment. The results demonstrate that in environments supplemented with IL-2, eCAR-NK and traditional CAR-NK, both targeting specific antigens, exhibit comparable cytotoxic activities (Fig. 3a-d). However, in conditions devoid of IL-2, eCAR-NK continue to exhibit substantial cytotoxicity, while the cytotoxic capacity of traditional CAR-NK is significantly diminished (Fig. 3a-d). Additionally, eCAR-NK cells do not exhibit increased non-specific cytotoxic

activity compared to CAR-NK cells. Against MSLN-knockout AsPC-1 cells, both eCAR-NK and CAR-NK display similar and relatively low cytotoxic activities (Extended Data Fig. 3a). Intriguingly, it was observed that eCAR-NK were uniquely capable of secreting the cytotoxic effector molecules interferon-γ (IFN-γ) and tumor necrosis factor-α (TNF-α) in the absence of IL-2 (Fig. 3e and Extended Data Fig. 3b).

We further explored the potential of eCAR to augment the *in vivo* antitumor efficacy of NK cells. Studies indicates that murine IL-15, with only 70% homology to human IL-15, fails to provide sufficient cytokine signaling for human NK cells (*12*). Thus, using Human IL-15 transgenic NCG mice (NCG-hIL15) and NCG mice can respectively simulate internal environments with sufficient and insufficient cytokines. Using the NCG-hIL15 mice, we established a Raji xenograft model of hematologic malignancy. After the adoptive transfer of effector cells for treatment, both CD19-specific eCAR-NK and CAR-NK significantly curtailed tumor progression and prolonged the survival of the tumor-bearing mice (Fig. 4a-c). To contrast these findings, we also established a Raji xenograft model in standard NCG mice, which lack human IL-15. In this model, only eCAR-NK cells demonstrated significant antitumor activity and notably extended the survival of tumor-bearing mice (Fig. 4d-f). Moreover, in solid tumor models, which possess more complex TME, eCAR-NK still exhibits robust antitumor activity (Fig. 4g-h). By examining the survival of adoptively transferred cells within the tumors, it was found that eCAR-NK could sustain proliferation over a 21-day observation period, whereas CAR-NK could not (Fig. 4i). Collectively, these results underscore that eCAR NK cells can effectively suppress tumor growth and enhance intratumoral survival, independent of cytokine support, and driven solely by tumor antigen recognition.

Integration of NKR Repertoire into eCAR Achieves Pan-Cancer Recognition

Considering the inherent heterogeneity and antigenic variability of solid tumors, we aimed to integrate an NKR repertoire into the eCAR to broaden the adoptive cells' recognition capabilities across a wide range of tumor antigens. We engineered eCAR by replacing the scFv to Ig-like domain of NKRs, facilitating the display of an NKR library (Fig. 5a, refer to it as eCAR-NKR library). It was found that various tumor stimuli could promote the proliferation of the eCAR-NKR library in the absence of exogenous cytokines (Fig. 5b). We summarized the NKRs and their corresponding ligands and examined the expression of NKR ligands on the surface of various tumor cells (Fig. 5c and Extended Data Fig. 4). Subsequently, we aimed to identify an eNKR from the eCAR-NKR library that could recognize pan-cancer. To achieve this, we stimulated the eCAR-NKR library with different tumor cells *in vitro* without exogenous cytokines and enriched eNKR. Ultimately, we discovered that NKG2D-eCAR NK cells

were consistently enriched under stimulation by various tumors (Fig. 5d-i).

eCAR-NKR improves antitumor effect target solid tumors

We proceeded to validate the antitumor efficacy of the eCAR-NKR library *in vivo* using various solid tumor mouse models, including GPC3-positive cancers (HepG2 and Huh-7), HER2-positive cancers (BT-474 and MKN45), and MSLN-positive pancreatic cancers (AsPC-1 and SK-OV-3). Post-treatment observations revealed that the eCAR-NKR library significantly curtailed tumor growth across these models (Fig. 6a-c). Furthermore, we established patient-derived tumor organoid xenograft (ODX) models to closely mimic clinical scenarios. The administration of the eCAR-NKR library to these ODX models effectively halted tumor progression, underscoring the library's potent therapeutic potential (Fig. 6d-e).

Discussion

Traditional CAR therapies, while effective in certain hematological malignancies, often falter in the face of solid tumors due to the complex TME and the diverse mechanisms of immune evasion employed by these cancers (*13, 14*). This study pioneers a novel chimeric receptor architecture, harnessing directed evolution, to concurrently deliver co-stimulatory and cytokine signals crucial for immune cell activation. This novel design facilitates NK cell proliferation in the absence of exogenous cytokines upon tumor antigen recognition. The receptor effectively transduces signals necessary for lymphocyte proliferation and activation, and by harnessing the NKR repertoire, it enables NK cells expressing this receptor to achieve broad-spectrum cytotoxicity against tumor cells. This receptor architecture effectively mitigates the suppressive TME characteristic of solid tumors, thereby substantially improving the survival and functionality of NK cells within the tumor tissue.

The capacity of eCAR-NK cells to operate autonomously, devoid of exogenous cytokines, underscores a pivotal advancement in adoptive cell therapy. Current strategies to ameliorate IL-2 signaling deficiencies within TME typically involve engineering adoptive cells to overexpress autocrine cytokines, thus sustaining their activation and proliferation (*15, 16*). While this approach proves effective, it harbors potential risks related to the physiological toxicity induced by cytokines. Furthermore, nutrient-scarce tumor environments impose a critical burden on adoptive cells' protein synthesis. Excessive cytokine production can precipitate endoplasmic reticulum stress due to heightened protein synthesis demands, potentially culminating in cellular dysfunction or death (*17*). The strategic design of eCAR addresses these challenges. By synthesizing eCARs primarily during ex vivo expansion, the adoptive cells utilize pre-formed molecules for IL-2 signal transduction upon reintegration into the tumor milieu,

minimizing cytokine-related adverse effects, thereby enhancing the viability of adoptive cell therapy for treating solid tumors (*15, 16*). Moreover, our results reveal that eCAR-NK cells not only proliferate upon co-cultivation with target cells but also specifically activate JAKs/STATs and AKT pathways upon antigen recognition—mirroring the dynamics of established IL-2 signaling cascades. This fidelity in signaling response further validates the efficacy and specificity of the eCAR design, positioning it as a formidable strategy in the landscape of cancer immunotherapy.

Utilizing the Ig-like domain of NKRs as a sensor for eCAR represents another innovative aspect of this study. Previous research has shown that many tumors express ligands for NKRs, and currently, the extracellular domains of NK receptors such as DNAM1 and NKp30 have been modified into chimeric receptors to enhance lymphocytes for antitumor therapy (*18, 19*). Despite this, adoptive cells modified in this way cannot avoid the issue of antigen loss. The combination of NKR with eCAR effectively addresses this problem. Upon entry into the body, the eCAR-NKR library expresses and different clones exhibit antigen-dependent proliferation, hindering tumor escape via antigen modulation. An interesting finding was the significant enrichment of NKG2D-eCAR across all *in vitro* stimulation experiments. This result also emphasizes the role of NKG2D as a universal receptor capable of recognizing multiple tumor-associated ligands. This type of single-receptor, multiple-target recognition molecule also provides a paradigm that can be learned for the development of artificial receptors in future synthetic biology.

Method

Cell lines HepG2, Huh-7, BT-474, MKN45, AsPC-1, SK-OV-3, Lenti-X 293T were obtained from the Shanghai Cell Bank (Chinese Academy of Sciences, Shanghai, China) and NK-92 was gifted by Dr. Huashun Li (Suzhou Institute of Systems Medicine). All cell lines were confirmed to be mycoplasma free. The cells were maintained in DMEM with 10% fetal bovine serum. Cell culture media and supplements were obtained from Life Technologies. NK-92 cell line was cultured as previously described (*20*).

Mice Female NOD/ShiltJGpt-*Prkdc*[em26Cd52]*Il-2rg*[em26Cd22]/Gpt (NCG) and NOD/ShiLtJGpt-*Prkdc*[em26Cd52]*Il2rg*[em26Cd22]*Il15*[em1Cin(hIL15)]/Gpt (NCG-hIL15) mice were obtained from Gempharmatech Inc (Nanjing, China) and housed under SPF facilities. Mice experiments were approved by the Scientific Investigation Board of Navy Medical University (Ethics Approval Number: 82471811).

Molecular Constructs Lentivirus vectors of pCDH-EF1-IRES-EGFP were designed and reconstructed. In which, transgene expression is driven by the EF1 promoter. Anti-CD19 antibody scFv (FMC63), hinge of CD8a, transmembrane domain of CD8, NKG2D, NKp44 and NKp46; cytoplasmic signaling domain of 4-1BB, and CD3ζ were

used to construct second-generation CARs; IL-2R ICDs are serially linked after CD3ζ or combined with negatively charged transmembrane regions from DAP10, DAP12, CD3ζ, or FcRγ, and then placed in parallel with second-generation CAR. Those gene fragments were synthesized by Tsingke company and cloned into the XbaI and NheI site of pCDH-EF1-IRES-EGFP using restriction enzyme cloning and ligation.

Western-blot Cells were lysed with cold lysis buffer (Cell Signaling Technology, Danvers, Massachusetts, U.S.) supplemented with protease inhibitor mixture (Calbiochem, Darmstadt, Germany). The total protein concentration was measured using the BCA assay (Pierce, Rockford, IL) and was equalized with the extraction reagent. Equivalent amounts of the extracts were loaded and subjected to 10% SDS–PAGE, transferred electrophoretically onto nitrocellulose membranes, and then analyzed by Western blotting.

Lentivirus Preparation and Cell Construction Lentivirus were generated using Lenti-X 293T cell line and packaging plasmid vectors. Twenty-four hours before transfection, 2×10^7 Lenti-X 293T cells were seeded in a 150-mm culture dish. Next, CAR-expression lentivirus vectors were transfected into packaging cells with psPAX2 and pMD2.G envelop plasmids, at a ratio of 4:3:1, using calcium-phosphate kit (ViralTherapy, R001) in accordance with the manufacturer's protocol. Supernatants were harvested after 48 and 72 h post-transfection and then they were concentrated by ultracentrifugation for 2.5 hours at 82,700 g at 4°C. Precipitated lentiviral particles were resuspended in Opti-MEM medium (Solarbio, 31985070). Lentiviral titer was determined using QuickTiter Lentivirus Quantitation Kit (Cell Biolabs, VPK-107) following the manufacturer's instructions. Stable cell lines were then established using lentivirus. Briefly, NK92 cells were seeded into 24-well plates at 1×10^5 cells/well, followed by infection with 2mg/mL polybrene (Yeasen, 40804ES76) at MOI=10. Finally, single clones were obtained by FACS sorting.

Immunofluorescence Cells grown on coverslips were incubated with anti-ATRX (Sigma HPA001906), antibodies and secondary antibodies conjugated with Alexa Fluor 488 and 594 (Molecular Probes). Nuclei were counterstained with Hoechst 33342 and slides were mounted in ProLong Gold (Molecular Probes). Images were acquired on a Zeiss LSM780 confocal microscope using a 40X objective, 2X internal magnification and an optimum voxel size determined by the Zeiss Zen software. Maximum intensity projections of Z-stacks are shown (*21*).

Cytotoxicity Assays NK cells to tumor cells cytotoxicity assays were determined by the extracellular release of lactate dehydrogenase (LDH) using a CytoTox96 cytotoxicity assay kit (Promega, G1780) according to the manufacturer's instructions. Briefly, target cells were replated in NK cell media in white-walled 96-well plates, followed by the addition of NK cell at the indicated E:T ratios. Finally, cytotoxicity was

calculated based on LDH release using the following formula: Cytotoxicity (%) = $[LDH^{E:T}-LDH^{E}]/LDH^{Max}\times100\%$ (*22*).

Organoids culture We have successfully established and maintained cancer patient-derived organoids as previously reported (*23*). In the process, the tumor tissue was finely minced and subjected to enzymatic digestion using collagenase II at a concentration of 5 mg/mL, at a temperature of 37°C for a duration of one hour. Post digestion, the tissue was carefully embedded in Matrigel BME2 and nurtured in specific tumor organoid comprehensive human medium. The organoids' growth was meticulously documented using a DP73 microscope digital camera, capturing images at consistent positions to monitor their development.

Repeated stimulation assay NK cells were co-cultured with target cells at a 1:1 E:T ratio in a 24-well plate. NK cells were restimulated with fresh target cells every 36 hours and were counted before each addition of fresh stimulator cells.

Flow cytometry Specific steps as we previously described (*24*). Cell surface staining was performed for 30 min at 4°C and samples were analysed using a FACSCalibur flow cytometer (BD Biosciences) and CellQuest Software (BD Biosciences). Cellular staining was performed for 60 min on ice after using a fixation/permeabilization kit (eBioscience). A minimum of 1×10^4 samples was examined.

Tumor-bearing mouse models and antitumor therapy For subcutaneous tumor model, tumor cells (5×10^6) were inoculated subcutaneously in the right flank of NCG mice. Tumors were established in mice and then treated with 1×10^7 NK cells via tail vein injection. Tumor volume was calculated by multiplying the tumor length and width three times a week, and mice reaching maximum tumor burden (15 mm in diameter) or exhibiting moribund signs were euthanized.

Next Generation Sequencing of CAR libraries Next Generation Sequencing was conducted to analyze the clone enrichment of NKR-eCAR libraries. After coculturing the library with tumor cells, collect the EGFP-positive NK cells and extract DNA for PCR amplification and sequencing of the inserted fragment to determine the NKR. The PCR primers are: F: 5'-GATTACAAGGATGACGACGATAA-3', R: 5'-GACAGGGGCTGCGACG-3'.

Statistical analysis Unless otherwise specified, Student's t-test was used to evaluate the significance of differences between 2 groups, and analysis of variance (ANOVA) was used to evaluate differences among 3 or more groups. Survival analysis was performed by Kaplan-Meier survival analysis. Differences between samples were considered significant when P<0.05.
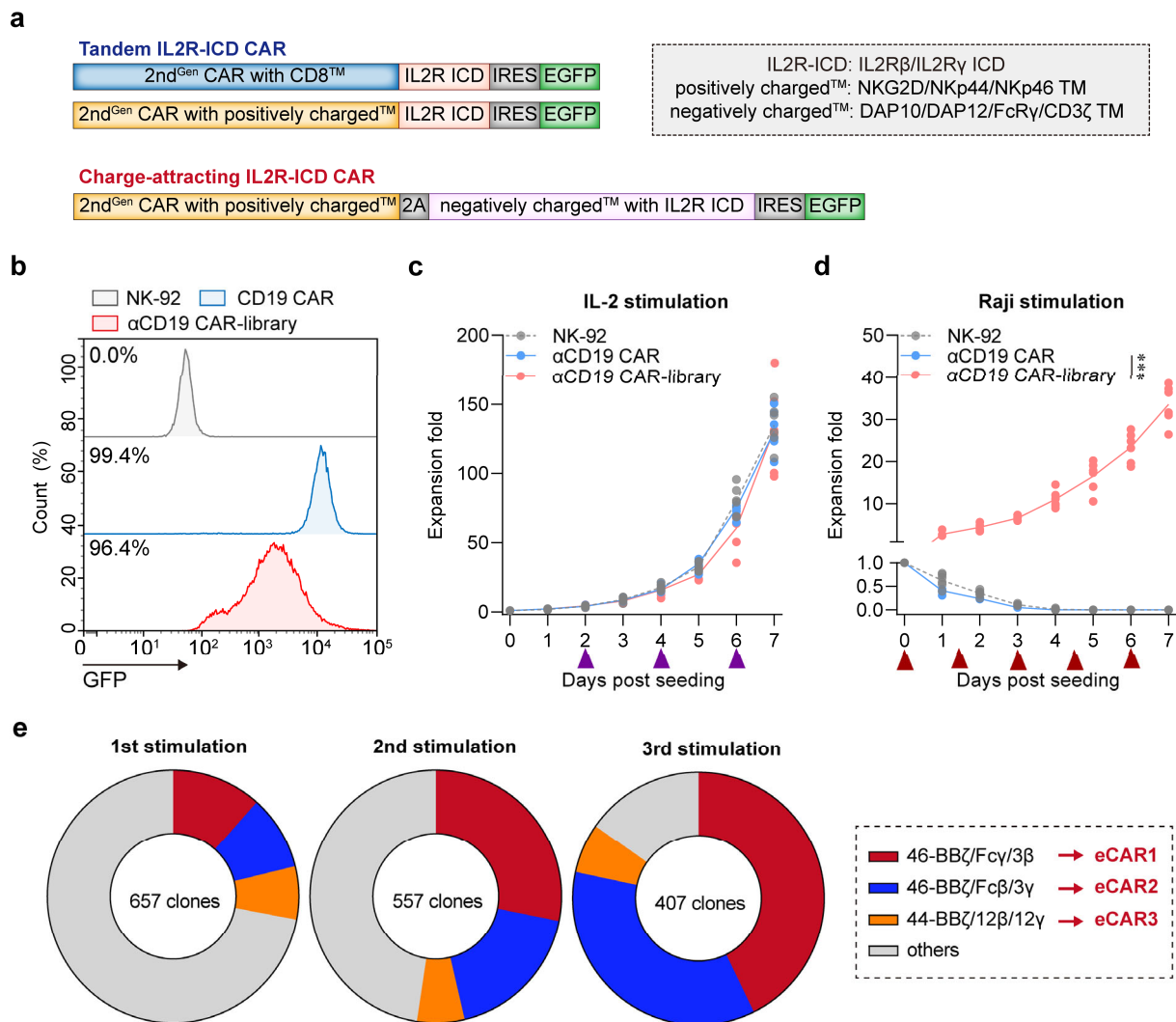
Figures

Fig. 1 | Design and verification of the synthetic CAR NK-92 cell library. a, Map of lentiviral constructs encoding the IL2R-ICD CAR library. **b,** Membrane-bound αCD19 CAR-library expression. At 72 h after retroviral transduction, the expression of αCD19 CAR-library on human NK-92 cells was measured by staining with anti-FLAG antibody, followed by flow cytometry analysis. NK-92 cells without transduction were used as negative controls. The histograms shown in grey correspond to the isotype controls and the blue histograms indicate positive fluorescence of αCD19 CAR, whereas the red histograms indicate positive fluorescence of αCD19 CAR-library. Data are representative of at least three independent experiments. **c-d,** Proliferation activity of CAR-NK cells in response to IL-2 and Raji stimulation (without IL-2). The purple arrow indicates the addition of an equal volume of fresh medium containing 100 IU/mL IL-2. The red arrow indicates the addition of an equal volume of fresh medium without IL-2, containing the same number of non-proliferative Raji cells (***$P < 0.001$ compared with NK-92). Data are presented as mean ± SD of six independent biological replicates. **e,** Growth dynamics of the αCD19 CAR-library in the periodical stimulation co-culture. Frequencies of αCD19 CAR-NK were analyzed before the addition of fresh target cells.
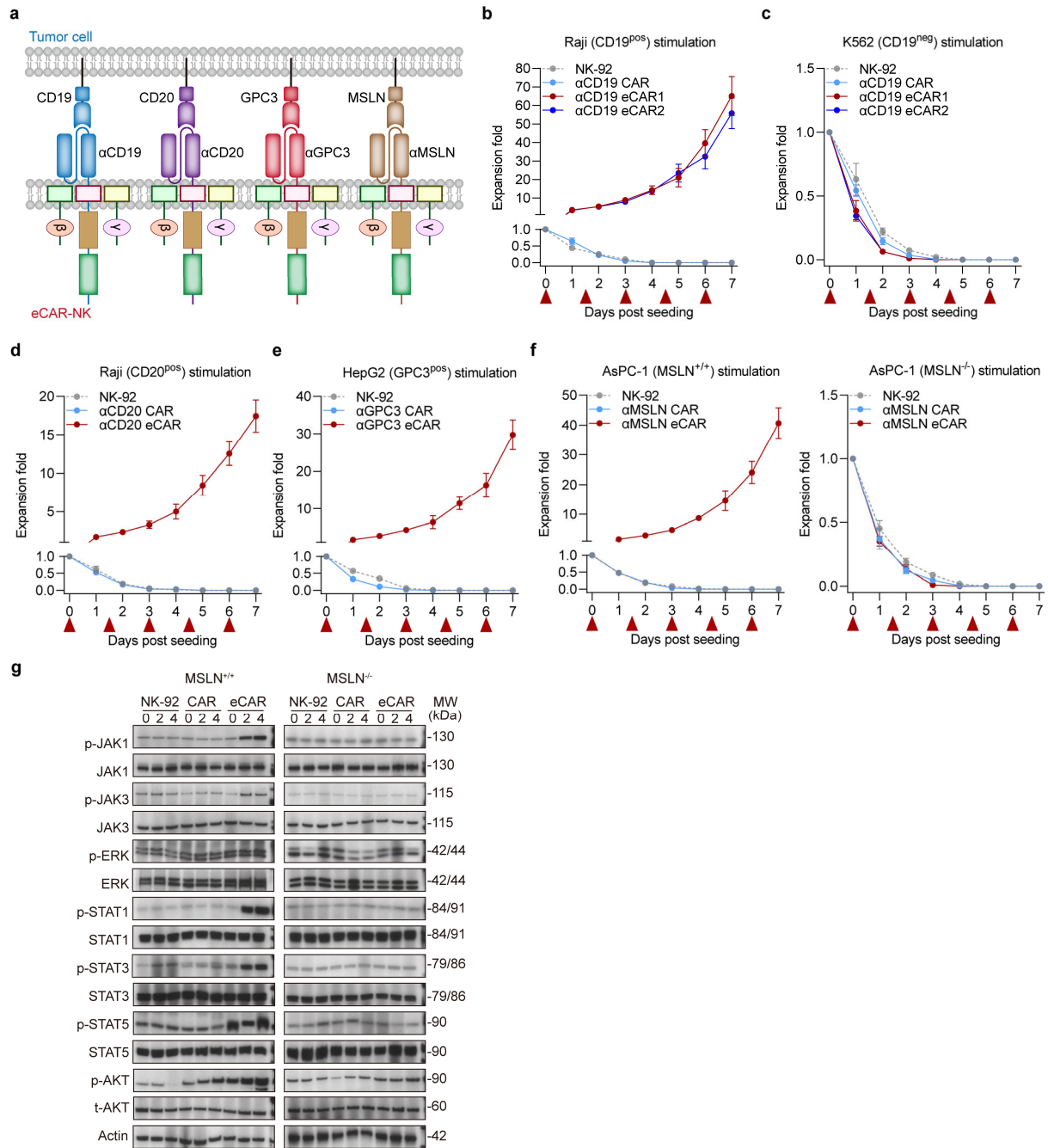
Fig. 2 | Proliferation activity of the eCAR NK-92 cells. a, Construction of four eCARs targeting different antigens (CD19, CD20, GPC3 and MSLN). **b-f,** Proliferation activity of eCAR NK-92 cells in response to tumor cells stimulation. Tumor cells treated with mitomycin C, including Raji (20 μM), K562(20 μM), HepG2 (30 μM) and AsPC-1 (30 μM). Data are presented as mean ± SD of five independent biological replicates. **g,** eCAR NK-92 cell activation pathway of JAK/STAT and MAPK indicated by Western Blot.
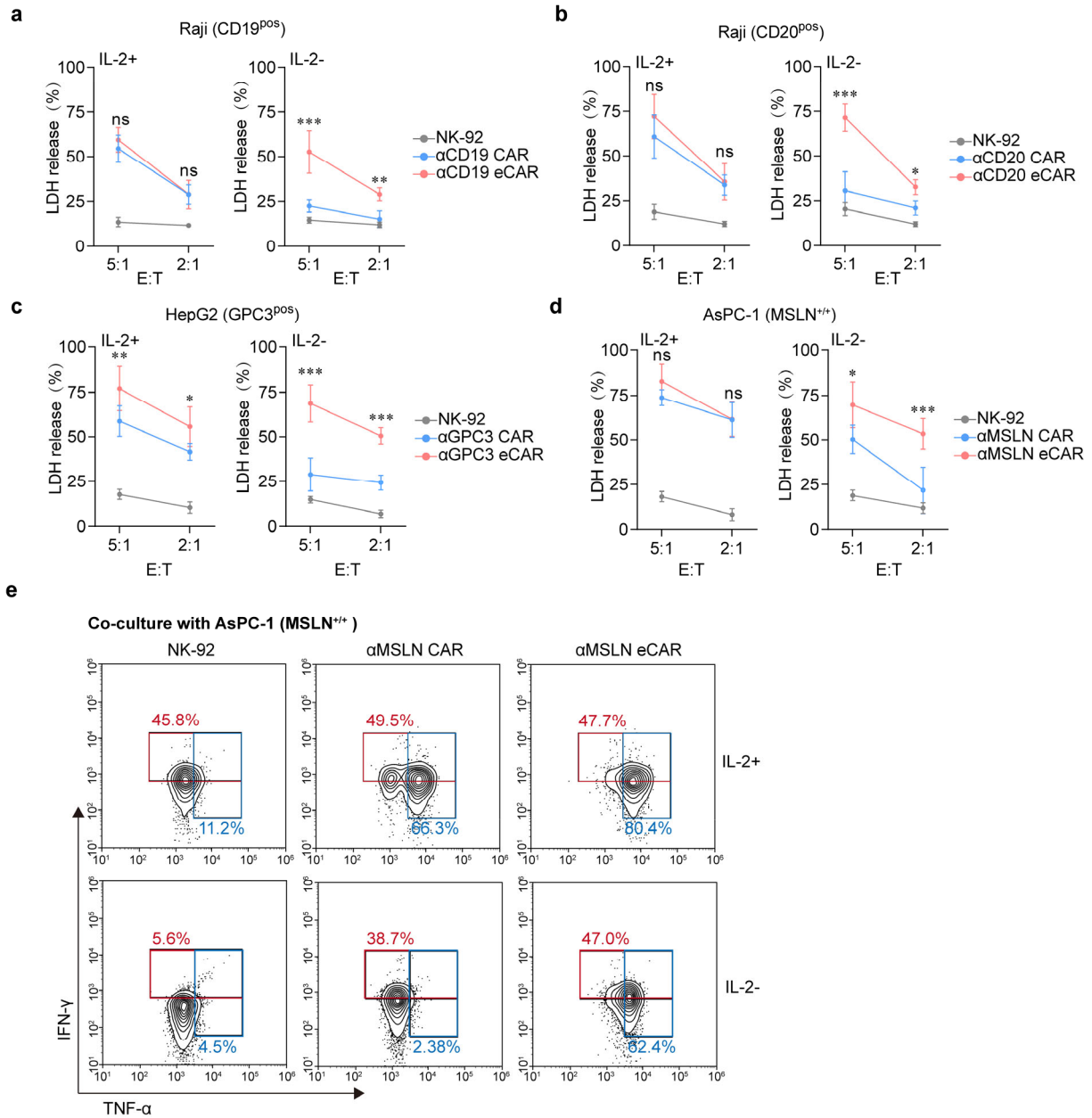
Fig. 3 | *In vitro* antitumor effect of the eCAR NK-92 cells. a-d, Cytotoxic activity of NK-92 (control), CAR or eCAR co-cultured with different tumor cells. Data were assessed by LDH Assay at the indicated E:T ratios and presented as mean ± SD of five independent biological replicates. (ns, not significant, *$P < 0.05$, **$P < 0.01$, ***$P < 0.001$ compared with NK-92). Data are mean ± SD. **e,** Killing activity of NK-92 (control), αMSLN CAR or αMSLN eCAR co-cultured with AsPC-1 (MSLN^{+/+}). The IFN-γ and TNF-α expression levels of eCAR NK-92 cells and the control NK cells against AsPC-1 (MSLN^{+/+}) under the condition of IL-2^{+} and IL-2^{−} were assessed by flow cytometry.
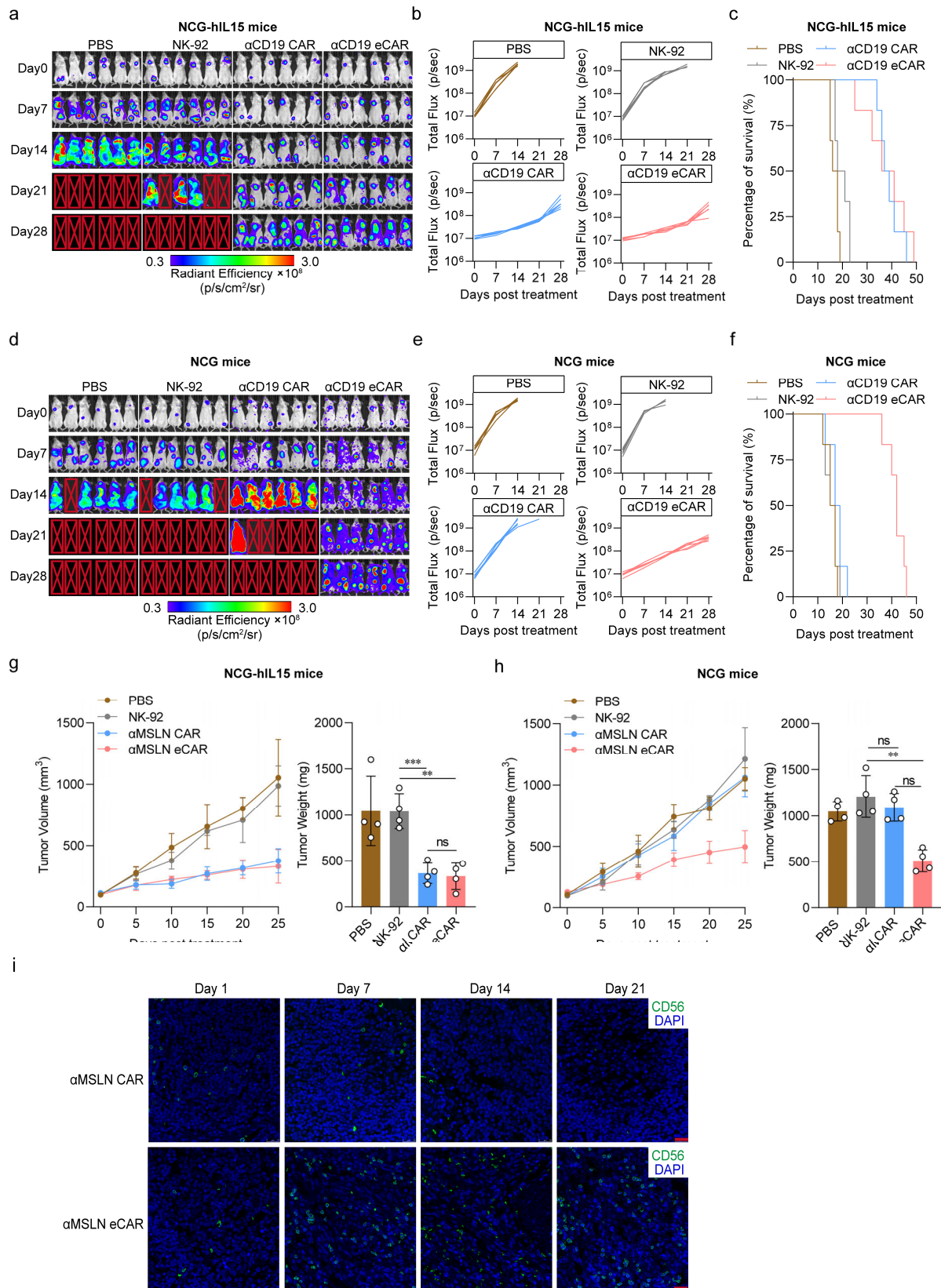
Fig. 4 | *In vivo* antitumor effect of the eCAR NK-92 cells. a, NCG-hIL15 mice were transplanted with Raji and the *in vivo* assess for tumor growth after treatment. The bioluminescence was monitored every 7 days. Image radiance values were normalized using Living Image (Perkinelmer) **b-c,** Tumor growth (**b**) and survival (**c**) of tumor-bearing mice treated with PBS (control), NK-92,

αCD19 CAR or αCD19 eCAR. **d,** NCG mice were transplanted with Raji and the *in vivo* assess for tumor growth after treatment. The bioluminescence was monitored every 7 days. Image radiance values were normalized using Living Image (Perkinelmer). **e-f,** Tumor growth (**e**) and survival (**f**) of tumor-bearing mice treated with PBS (control), NK-92, αCD19 CAR or αCD19 eCAR. **g-h,** Tumor volume and tumor weight of tumor-bearing mice treated with PBS (control), NK-92, αMSLN CAR or αMSLN eCAR (ns, not significant, **$P < 0.01$, ***$P < 0.001$ compared with NK-92). Data are mean ± SD. **i,** The eCAR NK-92 infiltration after treatment in subcutaneous pancreatic tumor biopsies was assess by immunofluorescence. The green fluorescence indicated the eCAR NK-92 cells and the blue fluorescence indicated DAPI, scale bar = 20 μm.
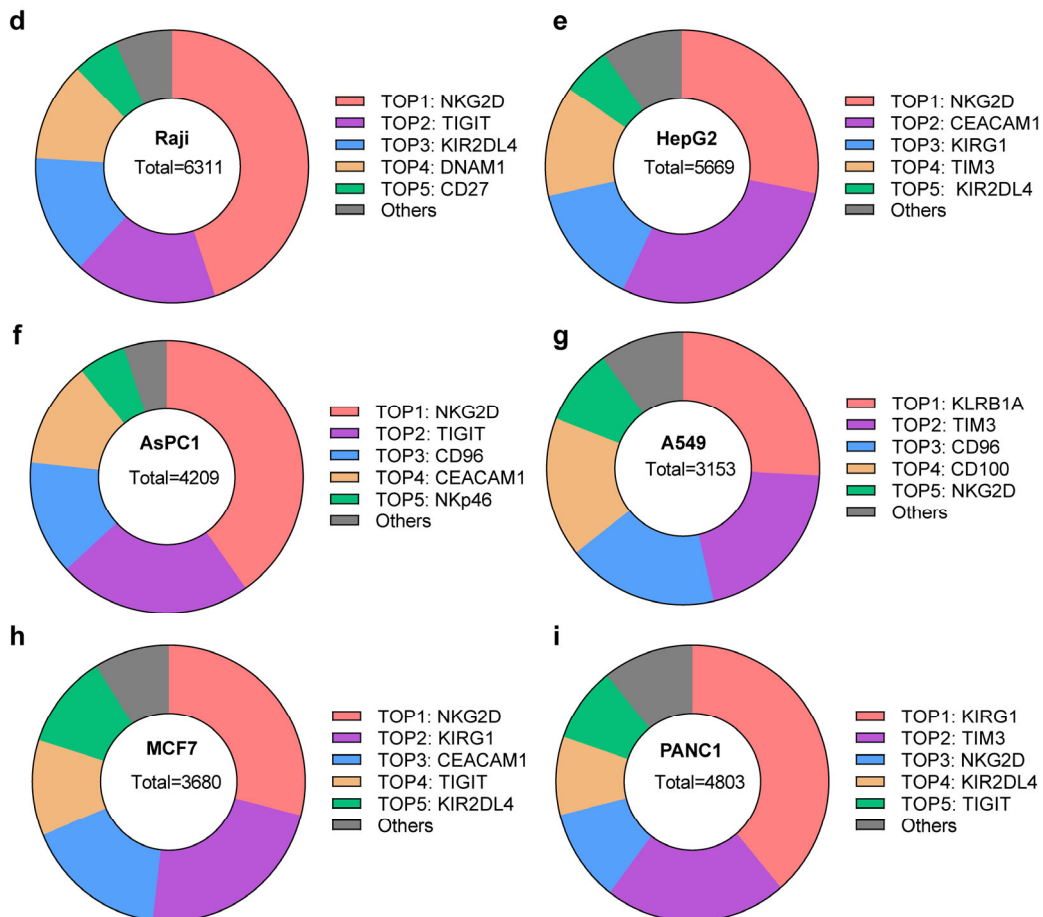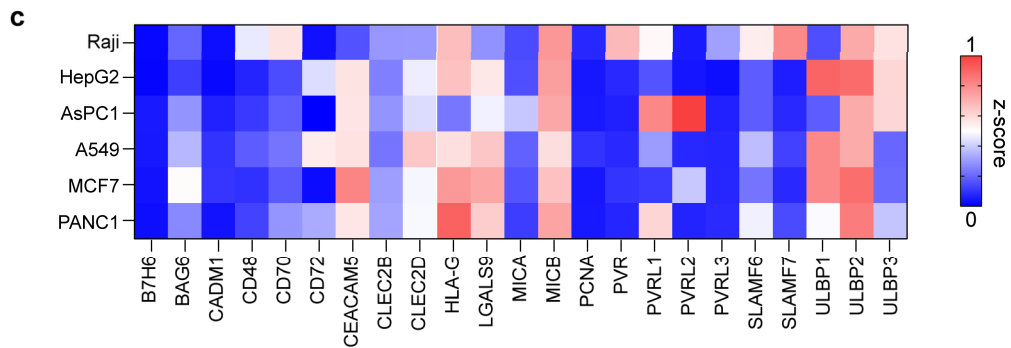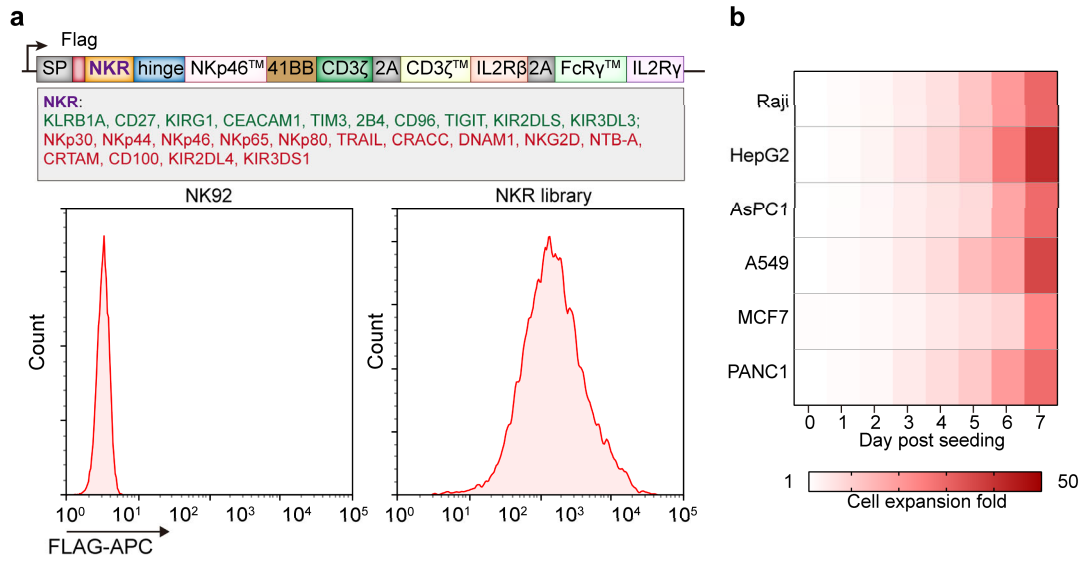
a

Flag

| SP | NKR | hinge | NKp46™ | 41BB | CD3ζ | 2A | CD3ζ™ | IL2Rβ | 2A | FcGγ™ | IL2Rγ |

NKR: KLRB1A, CD27, KIRG1, CEACAM1, TIM3, 2B4, CD96, TIGIT, KIR2DLS, KIR3DL3; NKp30, NKp44, NKp46, NKp65, NKp80, TRAIL, CRACC, DNAM1, NKG2D, NTB-A, CRTAM, CD100, KIR2DL4, KIR3DS1

b

Cell expansion fold 1 — 50

c

z-score 0 — 1

d Raji — Total=6311
- TOP1: NKG2D
- TOP2: TIGIT
- TOP3: KIR2DL4
- TOP4: DNAM1
- TOP5: CD27
- Others

e HepG2 — Total=5669
- TOP1: NKG2D
- TOP2: CEACAM1
- TOP3: KIRG1
- TOP4: TIM3
- TOP5: KIR2DL4
- Others

f AsPC1 — Total=4209
- TOP1: NKG2D
- TOP2: TIGIT
- TOP3: CD96
- TOP4: CEACAM1
- TOP5: NKp46
- Others

g A549 — Total=3153
- TOP1: KLRB1A
- TOP2: TIM3
- TOP3: CD96
- TOP4: CD100
- TOP5: NKG2D
- Others

h MCF7 — Total=3680
- TOP1: NKG2D
- TOP2: KIRG1
- TOP3: CEACAM1
- TOP4: TIGIT
- TOP5: KIR2DL4
- Others

i PANC1 — Total=4803
- TOP1: KIRG1
- TOP2: TIM3
- TOP3: NKG2D
- TOP4: KIR2DL4
- TOP5: TIGIT
- Others

Fig. 5 | Design and characterization of eCAR-NKR library. a, Construction of eCAR-NKR library. Map of lentiviral constructs encoding the eCAR-NKR library expression. At 72 h after retroviral transduction, the expression of eCAR-NKR library on human NK-92 cells was measured by staining with anti-FLAG antibody, followed by flow cytometry analysis. NK-92 cells without transduction were used as negative controls. The red histograms indicate positive fluorescence of eCAR-NKR library. Data are representative of at least three independent experiments. **b,** The expansion level of eCAR-NKR library in response to different tumor stimulations. **c,** The expression levels of different tumor ligands in different tumor cell lines. Data were normalized using z-score. **d-i,** The enrichment of eCAR-NKR library was assessed by NGS after stimulation of different tumor cells.
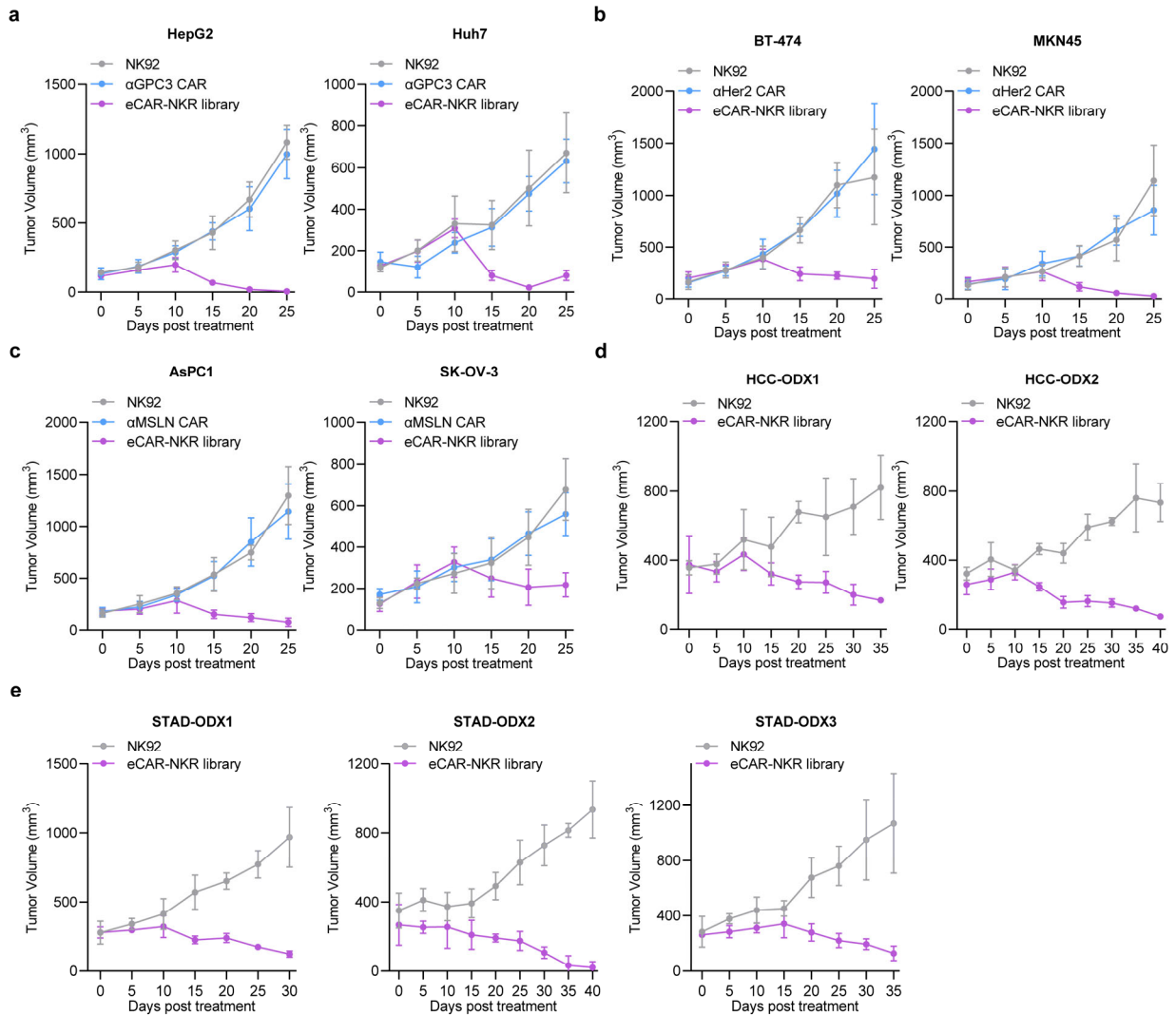
Fig. 6 | *In vivo* antitumor effect of the eCAR-NKR library. a, Tumor growth of tumor-bearing mice with GPC3-positive cancers (HepG2 and Huh-7) treated with NK-92 (control), αGPC3 CAR or eCAR-NKR library. **b,** Tumor growth of tumor-bearing mice with HER2-positive cancers (BT-474 and MKN45) treated with NK-92 (control), αHER2 CAR or eCAR-NKR library. **c,** Tumor growth of tumor-bearing mice with MSLN-positive pancreatic cancers (AsPC-1 and SK-OV-3) treated with NK-92 (control), αMSLN CAR or eCAR-NKR library. **d,** Tumor growth of tumor-bearing mice with two types of patient-derived tumor organoid xenografts (HCC) treated with NK-92 (control) or eCAR-NKR library. **e,** Tumor growth of tumor-bearing mice with three types of patient-derived tumor organoid xenografts (STAD) treated with NK-92 (control) or eCAR-NKR library. Data are presented as mean ± SD.

References

1. E. Liu *et al.*, Use of CAR-Transduced Natural Killer Cells in CD19-Positive Lymphoid Tumors. *N Engl J Med* **382**, 545-553 (2020).
2. Y. Gong, R. G. J. Klein Wolterink, J. Wang, G. M. J. Bos, W. T. V. Germeraad, Chimeric antigen receptor natural killer (CAR-NK) cell design and engineering for cancer therapy. *Journal of hematology & oncology* **14**, 73 (2021).
3. Y. Liu *et al.*, An Injectable Puerarin Depot Can Potentiate Chimeric Antigen Receptor Natural Killer Cell Immunotherapy Against Targeted Solid Tumors by Reversing Tumor Immunosuppression. *Small (Weinheim an der Bergstrasse, Germany)* **20**, e2307521 (2024).
4. V. Narayan *et al.*, PSMA-targeting TGFβ-insensitive armored CAR T cells in metastatic castration-resistant prostate cancer: a phase 1 trial. *Nature medicine* **28**, 724-734 (2022).
5. K. Beider *et al.*, Involvement of CXCR4 and IL-2 in the homing and retention of human NK and NK T cells to the bone marrow and spleen of NOD/SCID mice. *Blood* **102**, 1951-1958 (2003).
6. Y. Wang *et al.*, The IL-15-AKT-XBP1s signaling pathway contributes to effector functions and survival in human NK cells. *Nat Immunol* **20**, 10-17 (2019).
7. Q. Ma *et al.*, A PD-L1-targeting chimeric switch receptor enhances efficacy of CAR-T cell for pleural and peritoneal metastasis. *Signal transduction and targeted therapy* **7**, 380 (2022).
8. X. Hu, J. li, M. Fu, X. Zhao, W. Wang, The JAK/STAT signaling pathway: from bench to clinic. *Signal transduction and targeted therapy* **6**, 402 (2021).
9. Y. Li, D. L. Hermanson, B. S. Moriarity, D. S. Kaufman, Human iPSC-Derived Natural Killer Cells Engineered with Chimeric Antigen Receptors Enhance Anti-tumor Activity. *Cell stem cell* **23**, 181-192.e185 (2018).
10. J. D. Coudert, L. Scarpellino, F. Gros, E. Vivier, W. Held, Sustained NKG2D engagement induces cross-tolerance of multiple distinct NK cell activation pathways. *Blood* **111**, 3571-3578 (2008).
11. T. Igarashi *et al.*, Enhanced cytotoxicity of allogeneic NK cells with killer immunoglobulin-like receptor ligand incompatibility against melanoma and renal cell carcinoma cells. *Blood* **104**, 170-177 (2004).
12. C. Ju *et al.*, Human Interleukin 15 (IL15) Humanized NCG Mice Support the Human Natural Killer Cells Reconstitution and Development. *Blood* **134**, 4871-4871 (2019).
13. S. M. Poznanski *et al.*, Metabolic flexibility determines human NK cell functional fate in the tumor microenvironment. *Cell metabolism* **33**, 1205-1220. e1205 (2021).
14. D. Lindau, P. Gielen, M. Kroesen, P. Wesseling, G. J. Adema, The immunosuppressive tumour network: myeloid-derived suppressor cells, regulatory T cells and natural killer T cells. *Immunology* **138**, 105-115 (2013).
15. J. A. Myers, J. S. Miller, Exploring the NK cell platform for cancer immunotherapy. *Nat Rev Clin Oncol* **18**, 85-100 (2021).
16. A. Valeri *et al.*, Overcoming tumor resistance mechanisms in CAR-NK cell therapy. *Front Immunol* **13**, 953849 (2022).
17. C. Hetz, The unfolded protein response: controlling cell fate decisions under ER stress and beyond. *Nature Reviews Molecular Cell Biology*.
18. L. Cifaldi *et al.*, DNAM-1 chimeric receptor-engineered NK cells: a new frontier for CAR-NK cell-based immunotherapy. *Frontiers in Immunology* **14**, 1197053 (2023).

19. J. Quintin, S. M. Levitz, NKp30 enables NK cells to act naturally with fungi. *Cell Host & Microbe* **14**, 369-371 (2013).

20. C. Li, N. Yang, H. Li, Z. Wang, Robo1-specific chimeric antigen receptor natural killer cell therapy for pancreatic ductal adenocarcinoma with liver metastasis. *J Cancer Res Ther* **16**, 393-396 (2020).

21. Y. Liu *et al.*, Tumor exosomal RNAs promote lung pre-metastatic niche formation by activating alveolar epithelial TLR3 to recruit neutrophils. *Cancer cell* **30**, 243-256 (2016).

22. J. Wang *et al.*, Orthotopic and Heterotopic Murine Models of Pancreatic Cancer Exhibit Different Immunological Microenvironments and Different Responses to Immunotherapy. *Front Immunol* **13**, 863346 (2022).

23. L. Broutier *et al.*, Culture and establishment of self-renewing human and mouse adult liver and pancreas 3D organoids and their genetic manipulation. *Nat Protoc* **11**, 1724-1743 (2016).

24. Y. Han *et al.*, Tumor-induced generation of splenic erythroblast-like Ter-cells promotes tumor progression. *Cell* **173**, 634-648. e612 (2018).